

- Title page -

**Title:**

Metformin protects against sunitinib-induced cardiotoxicity: Investigating the role of AMPK

1

2 **Authors:**

3 Refik Kuburas, Ph.D.<sup>1</sup>, Mayel Gharanei, Ph.D.<sup>1</sup>, Irmgard Haussmann, Ph.D.<sup>1</sup>, Helen Maddock,  
4 Ph.D.<sup>1</sup>, Hardip Sandhu, PhD.<sup>1,\*</sup>

5

6 **Author affiliations:**

7 <sup>1</sup> Coventry University, Faculty Research Centre for Sport, Exercise and Life Sciences, Faculty of  
8 Health and Life Sciences, Alison Gingell Building, 20 Whitefriars Street, Coventry, CV1 2DS, United  
9 Kingdom

10

11 **\* Corresponding Author:**

12 Dr Hardip Sandhu

13 Coventry University, Faculty Research Centre for Sport, Exercise and Life Sciences, Faculty of  
14 Health and Life Sciences, Alison Gingell Building, 20 Whitefriars Street, Coventry, CV1 2DS, United  
15 Kingdom

16 Phone: +447506113009

17 email: hardip.sandhu@coventry.ac.uk

18

19 **Short running title:**

20 Metformin protects against sunitinib-induced cardiotoxicity

21

22 **Acknowledgments:**

23 None

24

25 **Funding:**

26 This research was supported by Coventry University, Faculty of Sport, Exercise and Life Sciences.

27

28 **Conflict of Interest:**

29 The authors have no conflicts of interest to declare that are relevant to the content of this article.

30

31

32

33  
34  
35  
36  
37  
38  
39  
40  
41  
42  
43  
44  
45  
46  
47  
48  
49  
50  
51  
52  
53  
54  
55  
56  
57  
58  
59

## **Abstract**

Sunitinib is associated with cardiotoxicity through inhibition of AMP-protein kinase (AMPK) signalling. In contrast, the common anti-diabetic agent metformin has demonstrated cardioprotection via indirect AMPK activation. Here we investigate the effects of metformin during sunitinib-induced cytotoxicity. Left ventricular developed pressure (LVDP), coronary flow (CF), heart rate (HR) and infarct size was measured in Langendorff perfused rat hearts treated with 1  $\mu$ M sunitinib  $\pm$  50  $\mu$ M metformin  $\pm$  1  $\mu$ M human equilibrative nucleoside transporter inhibitor S-(4-Nitrobenzyl)-6-thionosine (NBTI). Western blot analysis was carried out for p-AMPK $\alpha$  levels. Primary isolated cardiac myocytes from the left ventricular tissue were used to measure live cell population levels. 3-(4,5-dimethylthiazol-2-yl)-2,5-diphenyltetrazolium bromide (MTT) assay was used to assess adjunctive treatment of and metformin in human hepatoma G2 (HepG2) and promyelocytic leukaemia (HL-60) cells treated with 0.1-100  $\mu$ M sunitinib  $\pm$  50  $\mu$ M metformin. In the perfused hearts co-administration of metformin attenuated the sunitinib-induced changes to LVDP, infarct size and cardiac myocyte population. Western blot analysis revealed a significant decrease in p-AMPK $\alpha$  during sunitinib treatment, which was attenuated following co-administration with metformin. All metformin-induced effects were attenuated NBTI was co-administered. The MTT assay demonstrated an increase in the EC<sub>50</sub>-value during co-administration of metformin with sunitinib compared to sunitinib monotherapy in HepG2 and HL-60 cell lines, demonstrating the impact and complexity of metformin co-administration and the possible role of AMPK signalling. This study highlights the novel cardioprotective properties of metformin and AMPK activation during sunitinib-induced cardiotoxicity when administered together in the Langendorff heart model.

**Keywords:** Sunitinib, Metformin, AMP-protein kinase, Cardiotoxicity, Cardioprotection, Cardiac myocytes.

## **1 Introduction**

60 The multi-TKI sunitinib is used for the treatment of various cancers, including renal cell carcinoma,  
61 and as a second-line treatment for advanced gastrointestinal stromal tumour following imatinib  
62 resistance (1). However, the off-target effect of sunitinib can lead to serious cardiac dysfunction,  
63 such as hypertension, asymptomatic QT prolongation, reduction in left ventricular ejection fraction,  
64 acute coronary syndrome, myocardial infarction, and symptomatic congestive heart failure (2-5). The  
65 occurrence of congestive heart failure, myocardial injury, or cardiac death has been shown to be as  
66 high as 11 % in metastatic gastrointestinal stromal tumour patients treated with sunitinib (2).

67

68 Sunitinib-associated cardiac dysfunction is attributed to alterations in mitochondrial structure,  
69 including the induction of apoptosis and mitochondrial permeability transition pore (mPTP) opening,  
70 all of which contribute towards cardiac myocyte death and the induction of ischaemia (2, 6). Energy  
71 metabolism perturbations during pathological states such as ischaemia and cardiac hypertrophy  
72 activate the AMPK pathway inhibiting ATP-consuming anabolic pathways to conserve ATP and  
73 increase ADP levels (7-9), however, during sunitinib treatment the off-target AMPK signalling  
74 pathway is inhibited (4).

75

76 In the clinic metformin is used for the treatment of type 2 diabetes (10). Intracellularly metformin is  
77 known to inhibit the mitochondrial respiratory chain complex 1 in hepatocytes, which leads to a  
78 reduced cellular energy charge and an increase in the AMP/ATP ratio (11). This results in the  
79 activation of the AMPK pathway to facilitate glucose uptake in skeletal muscles, hepatocyte glucose  
80 production attenuation, and an increased level of free fatty acids oxidation (12, 13). Non-clinical and  
81 clinical studies have linked metformin with cardioprotective properties (14-16). The United Kingdom  
82 Prospective Diabetes study group showed that type 2 diabetes patients co-treated with metformin in  
83 addition to sulphonylurea had a 39% lower risk of developing myocardial infarction compared with  
84 conventional sulphonylurea mono-treatment (16). Multiple murine studies have shown that  
85 metformin administration, either before the ischaemic insult or at the moment of reperfusion,  
86 dramatically reduces the myocardial injury by activating the AMPK pathway, endothelial nitric oxide

87 synthase, and elevation of adenosine receptor stimulation (17-23). Moreover, the pre-conditioning  
88 effects of metformin involving AMPK activation further demonstrated that AMPK acts to regulate  
89 sarcolemmal  $K_{ATP}$  channels, indirectly of pathways associated with mitochondrial membrane  
90 potential (24, 25).

91

92 It is important to investigate if metformin offers cardioprotection during sunitinib-induced  
93 cardiotoxicity, and the role of AMPK during the metformin-induced cardioprotection in the whole  
94 heart, in cardiac myocytes, and at an intracellular level. Further to this, it is also imperative to  
95 investigate if metformin jeopardises the anti-proliferative properties of sunitinib in relevant cancer  
96 cell lines.

97

## 98 **2 Materials and Methods**

### 99 **2.1 Compliance with ethical standards**

100 Experiments were approved by Coventry University's ethics review board (project licence number  
101 P43367) according to Coventry University Policy and Standards (Animal Research: Reporting of *In*  
102 *Vivo* Experiments guidelines), which follows the United Kingdom Home office Guide on the  
103 Operation of the Animals (Scientific Procedures) Act 1986. Male Sprague–Dawley (SD) rats were  
104 used throughout this study due to general purpose model and based on previous worked carried out  
105 at Coventry University (26-28), and the housing and husbandry of the animals were followed as  
106 described previously by Andrag and Curtis (29). Studies of the animals were reported in compliance  
107 with the Animal Research: Reporting of *In Vivo* Experiments guidelines (30, 31). A total of 36  
108 animals were used for the Langendorff and triphenyl tetrazolium chloride (TTC) experimental model,  
109 49 for the western blot analysis and 7 for the cardiac myocyte experimental model

110

### 111 **2.2 Heart isolation prior to Langendorff and cardiac myocyte isolation**

112 For the Langendorff perfusion (n=6) and cardiac myocyte isolation (n=7) experiments male 2-3  
113 month old SD rats (Charles River laboratories, UK), weighing between 345-375 g, were selected at

114 random for each experimental group (i.e. vehicle, sunitinib, metformin, NBTI, sunitinib + metformin,  
115 and sunitinib + metformin + NBTI) (Sigma Aldrich, UK).

116

117 The rats were sacrificed by cerebral dislocation and their hearts were rapidly isolated and placed  
118 into ice cold 4°C Krebs-Henseleit (KH) bicarbonate buffer (NaCl 118.5 mM, NaHCO<sub>3</sub> 25.0 mM, KCL  
119 4.8 mM, MgSO<sub>4</sub> 1.2 mM, KH<sub>2</sub>PO<sub>4</sub> 1.2 mM, CaCl<sub>2</sub> 1.7 mM, glucose 11 mM, continuously gassed with  
120 95% O<sub>2</sub> and 5% CO<sub>2</sub> and maintained at pH 7.4±0.2 and 37±1°C). Hearts were immediately mounted  
121 onto the Langendorff perfusion system and cannulated via the aorta with a 1.4 mm inner diameter  
122 cannula, whilst retrogradely being perfused with KH buffer. The left atrium was trimmed away, and  
123 the latex isovolumic balloon was carefully introduced into the left ventricle and inflated up to 5–10  
124 mmHg end diastolic pressure. *Ex-vivo* perfused rat hearts were equilibrated and stabilised for 20  
125 min prior to starting the experiment. Functional recordings were measured using the physiological  
126 pressure transducer connected to a Bridge Amp and a PowerLab™ system (ADInstruments, UK).

127

### 128 **2.3 Langendorff perfusion protocol**

129 Sunitinib was administered at a concentration of 1 µM in accordance with steady state blood  
130 concentrations of sunitinib corresponding to 50 ng·ml<sup>-1</sup> in patients (1, 32). During previous work  
131 carried out by our team a concentration of 1 µM sunitinib have shown to induce cardiotoxicity in  
132 Langendorff perfused rat heart (26-28). Metformin was administered at a concentration of 50 µM in  
133 agreement to previous studies looking at the cardioprotective properties of metformin (17, 21). NBTI  
134 was administered at a concentration of 1 µM as previously studies using this concentration of NBTI  
135 had shown to inhibit the facilitated diffusion of adenosine through the human equilibrative nucleoside  
136 transporter, thus preventing the stimulation of the adenosine receptor to provide cardioprotection  
137 through the activation of AMPK (33). All drugs were dissolved in dimethyl-sulfoxide (DMSO) and  
138 sterile filtered using 5 µm pore size filters ensuring that the final DMSO concentration was <0.1 % in  
139 the perfusate KH bicarbonate buffer, as previously studies have shown that there are no changes in

140 contractility in cardiac *ex-vivo* experiments at this volume of DMSO in the KH bicarbonate buffer (26-  
141 28).

142

143 Hearts were perfused with at a constant pressure generated by the height of the perfusion column.

144 Hearts were stabilised with KH bicarbonate buffer for 20 min and excluded if pre-determined

145 exclusion criteria were met (i.e. CF: < 10 ml/min and > 28 ml/min; HR: < 70 beats/min and > 400

146 beats/min; LVDP: < 70 mmHg and > 130 mmHg) (34). LVDP, CF, and HR were measured at regular

147 intervals of 5 min for the first 20 min during stabilisation, intervals of 5 min for 35 min during initial

148 drug perfusion, and afterward at 15 min intervals for the remainder of 120 min drug perfusion (i.e. a

149 20 min stabilisation followed by a total of 155 min drug perfusion). During this study 1  $\mu$ M Sunitinib  $\pm$

150 50  $\mu$ M Metformin  $\pm$  1  $\mu$ M adenosine transporter inhibitor NBTI was administered through the KH

151 bicarbonate buffer perfusate following 20 min of stabilisation for each heart during the 155 min drug

152 perfusion. Control Langendorff hearts were perfused with vehicle. Following the Langendorff

153 perfusion experiment the left ventricular tissue was dissected free and the tissue was divided into

154 two portions for either TTC staining or Western blotting analysis.

155

## 156 **2.4 TTC staining**

157 Following Langendorff perfusion the hearts were dismantled, weighed, snap-frozen in liquid

158 nitrogen, and stored at -20°C. Frozen hearts were sliced into 2 mm thick transverse sections before

159 being incubated in TTC solution (1% concentration in phosphate buffer NaH<sub>2</sub>PO<sub>4</sub> 100 mM and

160 Na<sub>2</sub>HPO<sub>4</sub> 100 mM), at 37 $\pm$ 1°C for 10–12 min and fixed in 10% formalin for a minimum of 4 h. The

161 heart slices were monitored for discolouration and identity of the treatment group was kept

162 anonymous to reduce error and bias. Risk zone and infarct area were traced onto acetate sheets.

163 Computerised software ImageJ 1.52 (National Institutes of Health, USA) was used to analyse the

164 percentage of infarct tissue. Infarct size was normalised to the total area of each heart slice.

165

## 166 **2.5 Western blotting**

167 Following Langendorff perfusion the hearts were dismantled, and the left atrium coronary organ  
168 tissue was dissected, snap-frozen in liquid nitrogen, and stored in -80°C. The tissue was  
169 homogenised in Protein Lysis Buffer (tris-base, EDTA, SDS, NaCl, Sodium Pyruvate, NaF,  $\beta$ -  
170 glycerophosphate, protease inhibitor cocktail tablet and phosphostop tablet). A total of 60  $\mu$ g of protein  
171 concentration was determined using Pierce™ BCA Protein Assay Kit (Thermo Scientific, UK).  
172 Samples were mixed 1:1 with Laemmli buffer (tris-HCl, pH 6.8, SDS, glycerol,  $\beta$ -mercaptoethanol,  
173 and bromophenol blue ultra) and heated to 100°C. Samples were run using Mini-PROTEAN® TGX  
174 stain-free Gel™ (BioRad, UK), and were membrane transferred via electrophoresis with the Trans-  
175 Blot® Turbo™ Transfer (BioRad, UK). Immunoblots were incubated with 5 % bovine serum albumin  
176 powder in x1 concentration tris-buffered saline solution supplemented with tween for a 10 % tween  
177 concentration. Immunoblots were analysed using primary antibodies phosphorylated AMPK $\alpha$   
178 (1:1000 dilution, p-AMPK $\alpha$ , Thr<sup>172</sup>, #2531, RRID: AB\_330330, Cell Signalling Technologies, UK),  
179 and GAPDH (1:1000 dilution, D16H11, #5174, RRID:AB\_10622025, Cell Signalling Technologies,  
180 UK) for overnight incubation in 4°C followed by incubation with secondary antibody anti-rabbit IgG  
181 (1:1000 dilution, #7074, RRID: AB\_2099233, Cell Signalling Technologies, UK).  
182 Chemiluminescence detection kit SuperSignal™ West Femto Maximum Sensitivity Substrate  
183 (Thermo Scientific, UK) was used to visualise membranes. Images were taken using ChemiDoc™  
184 System (BioRad, UK). Density was analysed with the software Quantity One® (BioRad, UK).  
185 Analysis of p-AMPK $\alpha$  protein receptor bands was normalised to GAPDH and quantified using  
186 ImageJ 1.52 (National Institutes of Health, USA). Bands were analysed for the following treatment  
187 groups; vehicle (n=7), metformin (n=7), sunitinib (n=6), metformin + sunitinib (n=7), NBTI (n=7) and  
188 metformin + sunitinib + NBTI (n=7).

189

## 190 **2.6 Cardiac myocyte isolation and trypan blue staining**

191 Rat left ventricular cardiac myocytes were isolated by conventional enzymatic dissociation.  
192 Following cerebral dislocation the rat hearts were immediately isolated and mounted onto a modified  
193 Langendorff apparatus. Hearts were perfused with *modified* KH bicarbonate buffer (116 mM NaCl,



194 5.4 mM KCl, 0.4 mM MgSO<sub>4</sub>·7H<sub>2</sub>O, 10 mM Glucose, 20 mM Taurine, 5 mM Pyruvate, 2.4 mM  
195 NaHCO<sub>3</sub> and 12 mM KH<sub>2</sub>PO<sub>4</sub>, continuously gassed with 95% O<sub>2</sub> and 5% CO<sub>2</sub> and maintained at pH  
196 7.4±0.2 and 37±1°C) for stabilisation followed by perfusion with collagenase buffer (pH 7.4±0.2, 1  
197 mg·mL<sup>-1</sup> Type II collagenase powder, 1 M CaCl<sub>2</sub>) in *modified* KH buffer. The effluent was collected  
198 and reused following perfusion, the rat hearts were dismantled, and the atrium was cut away  
199 following completion of cardiac myocyte isolation. Left ventricular tissue was manually dissociated in  
200 collagenase buffer. Following centrifugation and removal of supernatant the pellet was redistributed  
201 in restoration buffer prepared in *modified* KH bicarbonate buffer at pH 7.4±0.2, containing 1%  
202 Bovine Serum Albumin, 1% pen-strep, creatine, and 100 mM CaCl<sub>2</sub>. The calcium concentration was  
203 gradually brought back to 1.25 mM and the myocyte viability was assessed under light microscopy.  
204 Cardiac myocytes were seeded and incubated for 4 h in 37±1°C with vehicle, 1 µM sunitinib ± 50 µM  
205 metformin ± 1 µM NBTI prior to undergoing trypan blue (0.4% w·v<sup>-1</sup> in 1x PBS filtered, 1:1 dilution,  
206 2x concentration) staining for assessment of live cell population counts.

207

## 208 **2.7 Cancer cell lines experimental protocol**

209 HepG2 (n=6) and HL-60 (n=6) cells were investigated for assessing cell metabolic activity with  
210 nicotinamide adenine dinucleotide phosphate dependent cellular oxidoreductase enzymes to reduce  
211 tetrazolium dye MTT to the insoluble formazin product. Experiments were performed using HepG2  
212 (RRID: CVCL\_0027) and HL-60 (CVCL\_0002) cell lines acquired from The American Type Culture  
213 Centre and brought up from at Coventry University in accordance with Coventry University ethical  
214 approval procedures. Sunitinib is used to treat leukaemia by inhibiting the overactive BCR-ABL  
215 tyrosine kinase detected during acute myeloid leukaemia (35), therefore the HL-60 cell line was  
216 deemed as a suitable model to investigate the cytotoxic properties of sunitinib. Moreover HepG2 cell  
217 line was deemed suitable for a comparison study to investigate the potential anti-proliferative  
218 properties with metformin in the treatment of liver carcinoma but also in alignment with studies  
219 demonstrating sunitinib for treatment of hepatocellular carcinoma (36). HepG2 and HL-60 cell lines  
220 were incubated with 0.1-100 µM Sunitinib ± 50 µM Metformin for 24 h (37 °C, 5% CO<sub>2</sub>) prior to the

221 media being replaced with MTT solution (concentration 5 mg·mL<sup>-1</sup> in sterile x1 concentration PBS)  
222 for 6 h. Media containing MTT solution was aspirated and replaced with DMSO prior to plates being  
223 read on a microtiter plate reader at 595 nm (reference 690 nm). Metformin mono-treatment in  
224 concentrations of 6 µM – 1 mM in HepG2 and 30 µM – 1 mM in HL-60 cells was also investigated.

225

## 226 **2.8 Data and statistical analysis**

227 Data are presented as means ± SEM. Statistical comparisons of a single variable was analysed by  
228 one way ANOVA with LSD post hoc test between vehicle ± sunitinib ± metformin ± NBTI using  
229 GraphPad Prism. Values of p < 0.05 were considered statistically significant. In the cancer cell lines  
230 the EC<sub>50</sub>-values of the sunitinib ± metformin dose-response curves were determined using  
231 GraphPad Prism.

232

## 233 **2.9 Drugs and materials**

234 Sunitinib malate (PZ0012-25 mg), Metformin hydrochloride (PHR1084-500 mg), and S-(4-  
235 Nitrobenzyl)-6-thionosine (NBTI) (N2255-100 mg) and 3-(4,5-dimethylthiazol-2-yl)-2,5-  
236 diphenyltetrazolium bromide (MTT) (M2128-250 mg) were purchased from Sigma Aldrich (Merck),  
237 UK. Phospho-AMPKα (Thr172) (#2531, RRID:AB\_330330), Total AMPKα (Cat:#2532,  
238 RRID:AB\_330331), GAPDH (Cat:#5174, RRID:AB\_10622025) and anti-rabbit IgG HRP-linked  
239 (Cat:#7074, RRID:AB\_2099233) were purchased from Cell Signalling Technologies, UK. The  
240 western blots kits Mini-PROTEAN® TGX stain-free Gel™ and Trans-Blot® Turbo™ Transfer were  
241 purchased from BioRad, UK, while Pierce™ BCA Protein Assay Kit and SuperSignal™ West  
242 Femto Maximum Sensitivity Substrate were from Thermo Fisher Scientific, UK.

243

## 244 **3 Results**

245 **3.1 Metformin co-administration attenuates sunitinib-induced changes in LVDP through**  
246 **AMPK in the perfused heart**

247 Measurements of LVDP, CF, and HR were carried out to investigate the role of sunitinib and  
248 metformin adjuvant therapy in Langendorff perfused rat hearts. Sunitinib administration significantly  
249 decreased LVDP compared to vehicle perfused hearts at the selected time-points: 145 min (vehicle  
250 =  $79.6 \pm 3.3\%$  vs. sunitinib =  $63.6 \pm 5.2\%$ ), 160 min (vehicle =  $78.6 \pm 3.7\%$  vs. sunitinib =  $57.4 \pm 5.6\%$ ),  
251 and 175 min (vehicle =  $77.2 \pm 3.3\%$  vs. sunitinib =  $58.3 \pm 5.9\%$ ). Co-administration of sunitinib and  
252 metformin perfusion in hearts significantly attenuated the sunitinib-induced decrease in LVDP at the  
253 same selected time-points mentioned above: 145 min (sunitinib =  $63.6 \pm 5.2\%$  vs. sunitinib +  
254 metformin =  $80.1 \pm 5.6\%$ ), 160 min (sunitinib =  $57.4 \pm 5.6\%$  vs. sunitinib + metformin =  $75.1 \pm 3.4\%$ ),  
255 and 175 min (sunitinib =  $58.3 \pm 5.9\%$  vs. sunitinib + metformin =  $73.9 \pm 3.5\%$ ). To investigate the role  
256 of intracellular adenosine needed for AMPK signalling during metformin-induced cardioprotection,  
257 NBTI was added to the perfusate containing sunitinib and metformin throughout the Langendorff  
258 experiments. The co-administration of sunitinib and metformin with NBTI during perfusion  
259 significantly attenuated the metformin-induced restoration of LVDP again at the specific time-points  
260 highlighted above: 145 min (sunitinib + metformin =  $80.1 \pm 5.6\%$  vs. sunitinib + metformin + NBTI =  
261  $65.4 \pm 3\%$ ), 160 min (sunitinib + metformin =  $75.1 \pm 3.4\%$  vs. sunitinib + metformin + NBTI =  
262  $64.01 \pm 1.63\%$ ), and 175 min (sunitinib + metformin =  $73.9 \pm 3.5\%$  vs. sunitinib + metformin + NBTI =  
263  $63.73 \pm 2.28\%$ ) (Figure 1A). Sunitinib administration did not significantly decrease CF when  
264 compared to vehicle perfused hearts, however, the co-administration of metformin and sunitinib  
265 significantly reduced CF compared to vehicle perfused hearts at the selected time points: 145 min  
266 (vehicle =  $80.8 \pm 4\%$  vs. sunitinib + metformin =  $70.1 \pm 4\%$ ), 160 min (vehicle =  $79.9 \pm 4\%$  vs. sunitinib +  
267 metformin =  $65.3 \pm 3.3\%$ ), and 175 min (vehicle =  $77.8 \pm 2.7\%$  vs. sunitinib + metformin =  $58.9 \pm 3.5\%$ ).  
268 The addition of NBTI with sunitinib and metformin significantly decreased the CF compared to  
269 sunitinib and metformin co-administered hearts at the selected time-points: 100 min (sunitinib +  
270 metformin =  $80.3 \pm 3.3\%$  vs. sunitinib + metformin + NBTI =  $59.3 \pm 6.8\%$ ), 115 min (sunitinib +  
271 metformin =  $76.2 \pm 4.6\%$  vs. sunitinib + metformin + NBTI =  $56.5 \pm 6.4\%$ ), 130 min (sunitinib +  
272 metformin =  $74.7 \pm 4.4\%$  vs. sunitinib + metformin + NBTI =  $54.8 \pm 5.5\%$ ), 145 min (sunitinib +  
273 metformin =  $70.1 \pm 4.0\%$  vs. sunitinib + metformin + NBTI =  $52.2 \pm 6.6\%$ ), 160 min (sunitinib +

274 metformin =  $65.3 \pm 3.3\%$  vs. sunitinib + metformin + NBTI =  $47.7 \pm 6.4\%$ ), and 175 min (sunitinib +  
275 metformin =  $58.9 \pm 3.5\%$  vs. sunitinib + metformin + NBTI =  $39.5 \pm 5.2\%$ ) (Figure 1B). The  
276 administration of sunitinib and metformin did not significantly alter the HR when compared to vehicle  
277 perfused hearts (Figure 1C).

278

### 279 **3.2 Metformin protects the perfused heart from sunitinib-induced infarction through AMPK**

280 To determine the potential cardioprotective properties of metformin following co-administration with  
281 Sunitinib, we assessed the infarct percentage of rat heart tissue following the Langendorff perfusion  
282 using TTC staining. Sunitinib perfusion of hearts resulted in a significant increase in infarct size  
283 percentage when compared to vehicle perfused control hearts (vehicle =  $11.4 \pm 0.5\%$  vs. sunitinib =  
284  $31.3 \pm 2.1\%$ ). The sunitinib-induced increase in infarct percentage was significantly attenuated  
285 following metformin co-administration with sunitinib (metformin + sunitinib =  $20.2 \pm 1.8\%$ ). Perfusion  
286 of NBTI together with sunitinib and metformin attenuated the metformin-induced decrease in infarct  
287 size, thus highlighting the involvement of AMPK and adenosine signalling in metformin-induced  
288 cardioprotection (sunitinib + metformin + NBTI =  $29.8 \pm 1.6\%$ ) (Figure 2).

289

### 290 **3.3 Sunitinib and metformin perfusion alters the level of p-AMPK $\alpha$ in the cardiac tissue**

291 To determine the involvement of AMPK signalling during metformin co-administration with sunitinib  
292 the level of p-AMPK $\alpha$  at Thr<sup>172</sup> was determined by Western blot analysis with SDS-PAGE using the  
293 left ventricular tissue obtained from the hearts following Langendorff perfusion. The p-AMPK $\alpha$  band  
294 intensities were normalised to vehicle and standardised against GAPDH band intensity levels. Here  
295 we demonstrate that p-AMPK $\alpha$  levels were decreased significantly following sunitinib perfusion of  
296 hearts when compared to vehicle perfused hearts (vehicle = 100% vs. sunitinib =  $56 \pm 10\%$ ).  
297 Metformin co-administration with sunitinib was able to significantly attenuate the decrease in p-  
298 AMPK $\alpha$  levels compared to sunitinib mono-treatment hearts (metformin + sunitinib =  $118 \pm 17\%$ ). The  
299 metformin-induced increase in p-AMPK $\alpha$  levels was significantly attenuated by co-administration

300 with NBTI along with sunitinib and metformin, which almost brought the p-AMPK $\alpha$  levels back to  
301 sunitinib mono-treatment levels (sunitinib + metformin + NBTI = 63 $\pm$ 13%) (Figure 3).

302

### 303 **3.4 Activation of AMPK prevents sunitinib-induced reduction in live cell population of** 304 **cardiac myocytes during co-administration with metformin**

305 Trypan blue staining of live cell population of isolated cardiac myocytes was used to demonstrate  
306 metformin's cardioprotective properties during incubation with sunitinib. Incubation with sunitinib was  
307 shown to significantly decrease the live cell population of isolated cardiac myocytes compared to  
308 vehicle (vehicle = 39.8 $\pm$ 3.6% vs. sunitinib = 11.6 $\pm$ 1.8%). Co-incubation of isolated cardiac myocytes  
309 with sunitinib and metformin significantly attenuated the decrease in live cell population induced by  
310 sunitinib mono-treatment (metformin + sunitinib = 41.3 $\pm$ 3.2%). To determine the role of AMPK  
311 during metformin-induced cardioprotection of isolated cardiac myocytes NBTI was incubated with  
312 sunitinib and metformin. This demonstrated a significant attenuation of metformin's cardioprotective  
313 effect during the sunitinib-induced cell death of isolated cardiac myocytes, highlighting the crucial  
314 involvement of the AMPK signalling pathway during metformin-induced cardioprotection (16.0 $\pm$ 3.0%)  
315 (Figure 4).

316

### 317 **3.5 Anti-neoplastic properties of sunitinib and metformin**

318 To determine if metformin jeopardised the anti-neoplastic properties of sunitinib HepG2 and HL-60  
319 cancer cell lines were treated with 50  $\mu$ M metformin in combination with 0.1-100  $\mu$ M sunitinib using  
320 the MTT assay. Sunitinib demonstrated a dose-dependent decrease in cell viability in HepG2 (EC<sub>50</sub>  
321 = 18.1  $\mu$ M) and HL-60 cells (EC<sub>50</sub> = 12.0  $\mu$ M) when standardised to vehicle treated cancer cells  
322 (Figure 5A-B). Compared to the vehicle group metformin mono-treatment did not alter cell viability of  
323 HepG2 cells (6  $\mu$ M – 1 mM metformin) or HL-60 cells (30  $\mu$ M – 1 mM metformin) (data not shown).  
324 Co-administration of 50  $\mu$ M metformin with sunitinib demonstrated a right-shift of the sunitinib dose-  
325 response curve, thus an increase in the EC<sub>50</sub> values for HepG2 (EC<sub>50</sub> = 43.6  $\mu$ M) and HL-60 cells  
326 (EC<sub>50</sub> = 27.6  $\mu$ M) was observed when compared to sunitinib mono-treatment (Figure 5A-B).

327

#### 328 **4 Discussion**

329 Our study demonstrates the novel adjunctive use of metformin together with sunitinib and the role of  
330 AMPK signalling during metformin-induced cardioprotection and sunitinib-induced cytotoxicity. In  
331 comparison to other studies that have used metformin and failed to demonstrate cardioprotection as  
332 pre-treatment (4, 37, 38), we highlight the significance and importance of co-administering  
333 metformin and activating AMPK signalling together with existing chemotherapeutic agents such as  
334 sunitinib in the Langendorff perfused animal heart model. Unlike studies by Cohen et al. 2011, we  
335 used a clinically relevant dose of sunitinib (1 $\mu$ M) in our animal heart study in order to closely monitor  
336 effects similar to patients receiving sunitinib (37). Metformin was administered for the same period of  
337 time as sunitinib, as well as adjunctively, in our *ex vivo* and *in vitro* models to closely monitor  
338 pleiotropic effects of metformin unlike studies by Cohen et al. 2011 and Hasinoff et al. 2008 who  
339 exposed cardiac cells for a shorter duration of time compared to sunitinib, but also removed  
340 metformin prior to exposing cardiac cells to sunitinib, which has the ability to inactivate AMPK once  
341 introduced (37, 38). For this reason, it did not make sense to remove the potential source of AMPK  
342 activation before administering toxicity. Our study highlights the potential for metformin to overcome  
343 sunitinib-mediated effects of AMPK signalling as indicated by the study conducted by Kerkela et al.  
344 2009 (4).

345

346 In this study, Langendorff perfusion of sunitinib significantly increased the infarct size and decreased  
347 LVDP in male SD rat hearts. In isolated cardiac myocytes sunitinib administration decreased live cell  
348 population. Western blotting analysis of the left ventricular tissue of sunitinib perfused hearts  
349 demonstrated a decrease in p-AMPK $\alpha$  signalling. Our findings on sunitinib-induced infarct increase  
350 and LVDP are supported by previous studies, where a similar decrease in whole rat heart sunitinib  
351 perfusion settings was observed (26-28). The observed changes in infarct size, LVDP, and cardiac  
352 myocytes cell viability following sunitinib administration in this study can be attributed to sunitinib  
353 initiating a pro-apoptotic response in cardiac myocytes (2, 6).

354

355 The inhibition of p-AMPK $\alpha$  by sunitinib treatment shown in this study is supported by previous  
356 studies involving *in vitro* and *in vivo* rodent experiments (3, 39). AMPK activation results in anti-  
357 apoptotic response to (a) promote mitochondrial biogenesis through PGC1- $\alpha$  and NRF1/2 gene  
358 expression stimulation to preserve mitochondrial homeostasis, (b) support the mitochondrial fission  
359 of oxidatively-damaged mitochondria through fission modulator dynamin-related protein 1 activation,  
360 and (c) preventing the opening of the mPTP (40). The decrease in p-AMPK $\alpha$  in our study can  
361 potentially be attributed to the sunitinib associated opening of the mPTP and mitochondrial  
362 dysfunction. AMPK is vital for cell survival during mitochondrial impairment, thus the inhibition of the  
363 AMPK pathway by sunitinib impairs energy homeostasis in cardiac myocytes and accelerate  
364 hypertrophy through release of eukaryotic elongation factor-2 and acetyl-coenzyme A carboxylase  
365 (3, 38). In the heart sunitinib-induced inhibition of ribosomal S6 kinase activity can trigger the  
366 release of pro-apoptotic factor BCL2-antagonist of cell death, leading to BCL2 associated X protein  
367 activation and cytochrome c release and activation of the intrinsic apoptotic pathway, resulting in  
368 ATP depletion, left ventricular dysfunction, and cardiac myocyte loss (3, 38). The cascade of these  
369 events contributes to mitochondrial impairment and dysfunction due to the sunitinib-induced  
370 cardiotoxicity (6). Therefore, another potential explanation for the reduction in LVDP and the  
371 reduction in p-AMPK $\alpha$  signalling in the left cardiac tissue following sunitinib perfusion could be due  
372 to the sunitinib-induced energy deprivation and ATP depletion, which could lead to a reduction in  
373 ATP availability for high energy-demanding cardiac myocytes (4). Further to this, p-AMPK $\alpha$  is vital in  
374 preventing cardiac myocyte death, as AMPK activation leads to activation of the catabolic pathway,  
375 suppressing non-essential ATP-consuming processes, thus re-distributing energy for cardiac  
376 myocyte and myocardium function (7, 41), and as a result of this sunitinib treatment reduces the  
377 cardiac myocyte cell viability and increases the infarct size in the whole heart.

378

379 Co-administration of metformin was able to abolish the cardiotoxic effects of sunitinib in the whole  
380 heart and in cardiac myocytes. Further to this, we demonstrated that the metformin associated

381 cardioprotective properties and the reactivation of p-AMPK $\alpha$  were attenuated by co-administration of  
382 NBTI. In line with the results demonstrated in this study, clinical studies have revealed that  
383 metformin therapy improves the survival outcome in diabetic patients suffering from metastatic renal  
384 cell carcinoma when treated with sunitinib when compared to metformin non-users (42, 43).  
385 Reperfusion studies using rat hearts subjected to regional ischemia and reperfusion showed a  
386 reduction in the myocardial infarct size through increased AMPK activation when 50  $\mu$ M metformin  
387 was administered during the first 15 min of reperfusion, with a 45% reduction in infarct size observed  
388 in SD rats (21), and a 34 % reduction in infarct size detected in Wistar rats, (22). Metformin's  
389 cardioprotective properties have been previously be attributed to attenuating the reperfusion-  
390 induced mPTP opening (17). There are no studies involving co-administration of metformin to  
391 prevent sunitinib-induced mPTP opening, however as previously noted, evidence exists of  
392 metformin-induced AMPK activation, which would lead to attenuation of the mPTP opening (40).  
393 Indeed studies have shown that the metformin-induced activation of AMPK signalling is required for  
394 the prevention of calcium-overload-mediated mPTP opening, mitochondrial oxidative  
395 phosphorylation, and the cascading pro-inflammatory response due to hypoxia, which are all the  
396 traits associated with cardiotoxicity (17, 44). In agreement with these studies metformin co-  
397 administration with sunitinib attenuated the sunitinib-mediated decrease in p-AMPK $\alpha$  levels in our  
398 study. Activation of AMPK signalling results in activation of endothelial nitric oxide synthase and  
399 nitric oxide bioavailability, thus preventing oxidative stress and apoptosis development (45-47).  
400 Metformin mediated increase in the AMP:ATP ratio levels facilitate the extracellular diffusion of  
401 adenosine via the equilibrative nucleoside transporter, which activates downstream cardioprotective  
402 pathways (48). The metformin-induced AMPK activation can be attenuated by inhibiting the  
403 equilibrative nucleoside transporter involved in the facilitated diffusion of adenosine across the  
404 cardiac myocyte cell membrane (33, 48). NBTI is demonstrated to attenuate intracellular adenosine  
405 signalling that results from metformin-induced increase in intracellular formation of adenosine by  
406 dephosphorylation of AMP (21, 35), the change in the ATP:AMP ratio and increase in cytosolic AMP  
407 signalling indirectly activates AMPK signalling (49-52). Previous studies demonstrated that free



408 adenosine in the cytosol provides a pivotal role in the formation of the endogenous purine  
409 nucleoside adenosine and acts to limit infarct size and mPTP formation (53, 54).

410

411 To investigate if metformin interfered with the anti-neoplastic properties of sunitinib, HepG2 and HL-  
412 60 cancer cell lines were incubated with sunitinib in the absence and presence of metformin.  
413 Sunitinib inhibited angiogenesis and induced a pro-apoptotic response in both HepG2 cells ( $EC_{50} =$   
414  $18.1 \mu\text{M}$ ) and HL-60 cells ( $EC_{50} = 12.0 \mu\text{M}$ ). Addition of  $50 \mu\text{M}$  metformin with increasing sunitinib  
415 doses resulted in a right-shift of the sunitinib dose-response curve, and thus an increase in  $EC_{50}$   
416 values (HepG2  $EC_{50} = 43.6 \mu\text{M}$  and HL-60  $EC_{50} = 27.6 \mu\text{M}$ ). These results from our study suggest  
417 that the activation of AMPK signalling may potentially reduce the sunitinib-induced ATP depletion in  
418 HepG2 and HI-60 cancer cells, and potentially protect cancer cells against oxidative stress and DNA  
419 damage (55). Even in the presence of metformin-induced activation of AMPK here we demonstrate  
420 that sunitinib still carries out anti-proliferative properties, indicating that sunitinib may be dependent  
421 on other intracellular pathways and mechanisms than an inactive AMPK pathway for its anti-cancer  
422 properties. Moreover, studies have shown that metformin has favourable effects on overall survival  
423 rates with sunitinib (43, 56), studies have shown that another multi-TKI sorafenib acts to activate  
424 AMPK (57) emphasise that activation of AMPK may not be the only cause of the metformin-induced  
425 right-shift and increase in  $EC_{50}$  values of the sunitinib dose-response curve observed in our study.  
426 The cause may lie with metformin's downstream targets, as metformin has been shown to suppress  
427 cisplatin-induced apoptotic cell death via an AMPK-independent manner, possibly by upregulation of  
428 the Akt survival pathway (58). In addition to metformin's cardioprotective properties, recent studies  
429 suggest that metformin has cytostatic effects in cancer cells rather than inducing apoptosis directly.  
430 Metformin was shown to reduce colony formation of colorectal cancer cells without arresting cell  
431 growth in the absence of apoptosis (59), and inhibition of AMPK did not prevent the metformin-  
432 induced anti-proliferative properties, but rather induced cell senescence by inhibiting the cell cycle at  
433 the  $G_0/G_1$  phase in a cytostatic manner (60). With this knowledge, the cytostatic effects of metformin  
434 to reduce cancer cell growth could compromise the cytotoxic effects of chemotherapeutic agents,

435 which would otherwise be more sensitive to more rapidly dividing cells. This highlights the  
436 complexity of adjunctive treatment with metformin. In order to further evaluate the role of metformin  
437 during sunitinib-induced cardiotoxicity a series of further *in vivo* experiments will be needed to be  
438 conducted in order to unravel the specific underlying pathways and mechanisms involved.

439

## 440 **5 Conclusion**

441 Sunitinib is associated with severe cardiotoxic adverse effects, thus identification of adjunctive  
442 therapy that will alleviate sunitinib-induced cardiotoxicity is vital for increasing the outcome in cancer  
443 patients treated with sunitinib. This study highlights metformin's potential cardioprotective property  
444 during sunitinib-induced cardiotoxicity. The sunitinib-induced increase in infarct size, decreases in  
445 LVDP, and decrease in isolated cardiac myocyte cell viability were attenuated by metformin co-  
446 administration, which was abolished by NBTI, thus emphasising on the involvement and importance  
447 of AMPK during metformin-induced cardioprotection. Importantly, metformin co-administration with  
448 sunitinib in relevant cancer cell lines did increase the EC<sub>50</sub> values. Our study highlights the  
449 complexity of adjunctive treatment and the fine balancing act of cardioprotection and treating  
450 carcinoma. Understanding the key intracellular pathways and mechanisms in both cardiac and  
451 cancer cells will unravel the potential of metformin as an adjunct therapy option in cancer patients  
452 treated with sunitinib.

453

## 454 **6 Reference list**

- 455 1. Goodman VL, Rock EP, Dagher R, Ramchandani RP, Abraham S, Gobburu JV, et al.  
456 Approval summary: sunitinib for the treatment of imatinib refractory or intolerant gastrointestinal  
457 stromal tumors and advanced renal cell carcinoma. Clin Cancer Res. 2007;13(5):1367-73.
- 458 2. Chu TF, Rupnick MA, Kerkela R, Dallabrida SM, Zurakowski D, Nguyen L, et al.  
459 Cardiotoxicity associated with tyrosine kinase inhibitor sunitinib. Lancet. 2007;370(9604):2011-9.

- 460 3. Force T, Krause DS, Van Etten RA. Molecular mechanisms of cardiotoxicity of tyrosine  
461 kinase inhibition. *Nat Rev Cancer*. 2007;7(5):332-44.
- 462 4. Kerkela R, Woulfe KC, Durand JB, Vagnozzi R, Kramer D, Chu TF, et al. Sunitinib-induced  
463 cardiotoxicity is mediated by off-target inhibition of AMP-activated protein kinase. *Clin Transl Sci*.  
464 2009;2(1):15-25.
- 465 5. Khakoo AY, Kassiotis CM, Tannir N, Plana JC, Halushka M, Bickford C, et al. Heart failure  
466 associated with sunitinib malate: a multitargeted receptor tyrosine kinase inhibitor. *Cancer*.  
467 2008;112(11):2500-8.
- 468 6. Gorini S, De Angelis A, Berrino L, Malara N, Rosano G, Ferraro E. Chemotherapeutic Drugs  
469 and Mitochondrial Dysfunction: Focus on Doxorubicin, Trastuzumab, and Sunitinib. *Oxid Med Cell*  
470 *Longev*. 2018;2018:7582730.
- 471 7. Dyck JR, Lopaschuk GD. AMPK alterations in cardiac physiology and pathology: enemy or  
472 ally? *J Physiol*. 2006;574(Pt 1):95-112.
- 473 8. Hardie DG, Carling D. The AMP-activated protein kinase--fuel gauge of the mammalian cell?  
474 *Eur J Biochem*. 1997;246(2):259-73.
- 475 9. Qi D, Young LH. AMPK: energy sensor and survival mechanism in the ischemic heart.  
476 *Trends Endocrinol Metab*. 2015;26(8):422-9.
- 477 10. Gottlieb B, Auld WH. Metformin in treatment of diabetes mellitus. *Br Med J*.  
478 1962;1(5279):680-2.
- 479 11. El-Mir MY, Nogueira V, Fontaine E, Averet N, Rigoulet M, Leverve X. Dimethylbiguanide  
480 inhibits cell respiration via an indirect effect targeted on the respiratory chain complex I. *J Biol*  
481 *Chem*. 2000;275(1):223-8.
- 482 12. Musi N, Hirshman MF, Nygren J, Svanfeldt M, Bavenholm P, Rooyackers O, et al. Metformin  
483 increases AMP-activated protein kinase activity in skeletal muscle of subjects with type 2 diabetes.  
484 *Diabetes*. 2002;51(7):2074-81.

- 485 13. Zhou G, Myers R, Li Y, Chen Y, Shen X, Fenyk-Melody J, et al. Role of AMP-activated  
486 protein kinase in mechanism of metformin action. *J Clin Invest.* 2001;108(8):1167-74.
- 487 14. Hausenloy DJ, Bhamra GS, Davidson SM, Carr R, Mocanu MM, Yellon DM. Metformin  
488 Cardioprotects the Diabetic Heart by Inhibiting mPTP Opening Via the Risk Pathway. *Journal of*  
489 *Molecular and Cellular Cardiology.* 2007;42(7).
- 490 15. Johnson JA, Majumdar SR, Simpson SH, Toth EL. Decreased mortality associated with the  
491 use of metformin compared with sulfonylurea monotherapy in type 2 diabetes. *Diabetes Care.*  
492 2002;25(12):2244-8.
- 493 16. UKPDS. Effect of intensive blood-glucose control with metformin on complications in  
494 overweight patients with type 2 diabetes (UKPDS 34). UK Prospective Diabetes Study (UKPDS)  
495 Group. *Lancet.* 1998;352(9131):854-65.
- 496 17. Bhamra GS, Hausenloy DJ, Davidson SM, Carr RD, Paiva M, Wynne AM, et al. Metformin  
497 protects the ischemic heart by the Akt-mediated inhibition of mitochondrial permeability transition  
498 pore opening. *Basic Res Cardiol.* 2008;103(3):274-84.
- 499 18. Calvert JW, Gundewar S, Jha S, Greer JJ, Bestermann WH, Tian R, et al. Acute metformin  
500 therapy confers cardioprotection against myocardial infarction via AMPK-eNOS-mediated signaling.  
501 *Diabetes.* 2008;57(3):696-705.
- 502 19. Charlon V, Boucher F, Mouhieddine S, de Leiris J. Reduction of myocardial infarct size by  
503 metformin in rats submitted to permanent left coronary artery ligation. *Diabetes Metabolism.*  
504 1988;14:591-5.
- 505 20. Legtenberg RJ, Houston RJ, Oeseburg B, Smits P. Metformin improves cardiac functional  
506 recovery after ischemia in rats. *Horm Metab Res.* 2002;34(4):182-5.
- 507 21. Paiva M, Riksen NP, Davidson SM, Hausenloy DJ, Monteiro P, Goncalves L, et al. Metformin  
508 prevents myocardial reperfusion injury by activating the adenosine receptor. *J Cardiovasc*  
509 *Pharmacol.* 2009;53(5):373-8.

- 510 22. Paiva MA, Goncalves LM, Providencia LA, Davidson SM, Yellon DM, Mocanu MM.  
511 Transitory activation of AMPK at reperfusion protects the ischaemic-reperfused rat myocardium  
512 against infarction. *Cardiovasc Drugs Ther.* 2010;24(1):25-32.
- 513 23. Solskov L, Lofgren B, Kristiansen SB, Jessen N, Pold R, Nielsen TT, et al. Metformin  
514 induces cardioprotection against ischaemia/reperfusion injury in the rat heart 24 hours after  
515 administration. *Basic Clin Pharmacol Toxicol.* 2008;103(1):82-7.
- 516 24. Sukhodub A, Jovanovic S, Du Q, Budas G, Clelland AK, Shen M, et al. AMP-activated  
517 protein kinase mediates preconditioning in cardiomyocytes by regulating activity and trafficking of  
518 sarcolemmal ATP-sensitive K(+) channels. *J Cell Physiol.* 2007;210(1):224-36.
- 519 25. Mohammed Abdul KS, Jovanovic S, Jovanovic A. Exposure to 15% oxygen in vivo up-  
520 regulates cardioprotective SUR2A without affecting ERK1/2 and AKT: a crucial role for AMPK. *J Cell*  
521 *Mol Med.* 2017;21(7):1342-50.
- 522 26. Cooper S, Sandhu H, Hussain A, Mee C, Maddock H. Ageing alters the severity of Sunitinib-  
523 induced cardiotoxicity: Investigating the mitogen activated kinase kinase 7 pathway association.  
524 *Toxicology.* 2019;411:49-59.
- 525 27. Cooper SL, Sandhu H, Hussain A, Mee C, Maddock H. Involvement of mitogen activated  
526 kinase kinase 7 intracellular signalling pathway in Sunitinib-induced cardiotoxicity. *Toxicology.*  
527 2018;394:72-83.
- 528 28. Sandhu H, Cooper S, Hussain A, Mee C, Maddock H. Attenuation of Sunitinib-induced  
529 cardiotoxicity through the A3 adenosine receptor activation. *Eur J Pharmacol.* 2017.
- 530 29. Andrag E, Curtis MJ. Feasibility of targeting ischaemia-related ventricular arrhythmias by  
531 mimicry of endogenous protection by endocannabinoids. *Br J Pharmacol.* 2013;169(8):1840-8.
- 532 30. Kilkeny C, Browne W, Cuthill IC, Emerson M, Altman DG, Group NCRREGW. Animal  
533 research: reporting in vivo experiments: the ARRIVE guidelines. *Br J Pharmacol.* 2010;160(7):1577-  
534 9.

- 535 31. McGrath JC, Lilley E. Implementing guidelines on reporting research using animals (ARRIVE  
536 etc.): new requirements for publication in BJP. *Br J Pharmacol.* 2015;172(13):3189-93.
- 537 32. Henderson KA, Borders RB, Ross JB, Huwar TB, Travis CO, Wood BJ, et al. Effects of  
538 tyrosine kinase inhibitors on rat isolated heart function and protein biomarkers indicative of toxicity. *J*  
539 *Pharmacol Toxicol Methods.* 2013;68(1):150-9.
- 540 33. Rose JB, Naydenova Z, Bang A, Eguchi M, Sweeney G, Choi DS, et al. Equilibrative  
541 nucleoside transporter 1 plays an essential role in cardioprotection. *Am J Physiol Heart Circ Physiol.*  
542 2010;298(3):H771-7.
- 543 34. Bell RM, Mocanu MM, Yellon DM. Retrograde heart perfusion: the Langendorff technique of  
544 isolated heart perfusion. *J Mol Cell Cardiol.* 2011;50(6):940-50.
- 545 35. Ikezoe T, Nishioka C, Tasaka T, Yang Y, Komatsu N, Togitani K, et al. The antitumor effects  
546 of sunitinib (formerly SU11248) against a variety of human hematologic malignancies: enhancement  
547 of growth inhibition via inhibition of mammalian target of rapamycin signaling. *Mol Cancer Ther.*  
548 2006;5(10):2522-30.
- 549 36. Koeberle D, Montemurro M, Samaras P, Majno P, Simcock M, Limacher A, et al. Continuous  
550 Sunitinib treatment in patients with advanced hepatocellular carcinoma: a Swiss Group for Clinical  
551 Cancer Research (SAKK) and Swiss Association for the Study of the Liver (SASL) multicenter  
552 phase II trial (SAKK 77/06). *Oncologist.* 2010;15(3):285-92.
- 553 37. Cohen JD, Babiarz JE, Abrams RM, Guo L, Kameoka S, Chiao E, et al. Use of human stem  
554 cell derived cardiomyocytes to examine sunitinib mediated cardiotoxicity and electrophysiological  
555 alterations. *Toxicol Appl Pharmacol.* 2011;257(1):74-83.
- 556 38. Hasinoff BB, Patel D, O'Hara KA. Mechanisms of myocyte cytotoxicity induced by the  
557 multiple receptor tyrosine kinase inhibitor sunitinib. *Mol Pharmacol.* 2008;74(6):1722-8.

558 39. Laderoute KR, Calaoagan JM, Madrid PB, Klon AE, Ehrlich PJ. SU11248 (sunitinib) directly  
559 inhibits the activity of mammalian 5'-AMP-activated protein kinase (AMPK). *Cancer Biol Ther.*  
560 2010;10(1):68-76.

561 40. Toyama EQ, Herzig S, Courchet J, Lewis TL, Jr., Loson OC, Hellberg K, et al. *Metabolism.*  
562 AMP-activated protein kinase mediates mitochondrial fission in response to energy stress. *Science.*  
563 2016;351(6270):275-81.

564 41. Allard MF, Parsons HL, Saeedi R, Wambolt RB, Brownsey R. AMPK and metabolic  
565 adaptation by the heart to pressure overload. *Am J Physiol Heart Circ Physiol.* 2007;292(1):H140-8.

566 42. Hamieh L, McKay RR, Lin X, Moreira RB, Simantov R, Choueiri TK. Effect of Metformin Use  
567 on Survival Outcomes in Patients With Metastatic Renal Cell Carcinoma. *Clin Genitourin Cancer.*  
568 2017;15(2):221-9.

569 43. Keizman D, Ish-Shalom M, Sella A, Gottfried M, Maimon N, Peer A, et al. Metformin Use and  
570 Outcome of Sunitinib Treatment in Patients With Diabetes and Metastatic Renal Cell Carcinoma.  
571 *Clin Genitourin Cancer.* 2016;14(5):420-5.

572 44. Wu S, Zou MH. AMPK, Mitochondrial Function, and Cardiovascular Disease. *Int J Mol Sci.*  
573 2020;21(14).

574 45. Davis BJ, Xie Z, Viollet B, Zou MH. Activation of the AMP-activated kinase by antidiabetes  
575 drug metformin stimulates nitric oxide synthesis in vivo by promoting the association of heat shock  
576 protein 90 and endothelial nitric oxide synthase. *Diabetes.* 2006;55(2):496-505.

577 46. Lefer AM. Attenuation of myocardial ischemia-reperfusion injury with nitric oxide replacement  
578 therapy. *Ann Thorac Surg.* 1995;60(3):847-51.

579 47. Wang XF, Zhang JY, Li L, Zhao XY, Tao HL, Zhang L. Metformin improves cardiac function  
580 in rats via activation of AMP-activated protein kinase. *Clin Exp Pharmacol Physiol.* 2011;38(2):94-  
581 101.

- 582 48. Bromage DI, Yellon DM. The pleiotropic effects of metformin: time for prospective studies.  
583 Cardiovasc Diabetol. 2015;14:109.
- 584 49. Bungler R, Soboll S. Cytosolic adenylates and adenosine release in perfused working heart.  
585 Comparison of whole tissue with cytosolic non-aqueous fractionation analyses. Eur J Biochem.  
586 1986;159(1):203-13.
- 587 50. Headrick JP, Willis RJ. 5'-Nucleotidase activity and adenosine formation in stimulated,  
588 hypoxic and underperfused rat heart. Biochem J. 1989;261(2):541-50.
- 589 51. Aymerich I, Fougelle F, Ferre P, Casado FJ, Pastor-Anglada M. Extracellular adenosine  
590 activates AMP-dependent protein kinase (AMPK). J Cell Sci. 2006;119(Pt 8):1612-21.
- 591 52. Zhang L, He H, Balschi JA. Metformin and phenformin activate AMP-activated protein kinase  
592 in the heart by increasing cytosolic AMP concentration. Am J Physiol Heart Circ Physiol.  
593 2007;293(1):H457-66.
- 594 53. Hausenloy DJ, Maddock HL, Baxter GF, Yellon DM. Inhibiting mitochondrial permeability  
595 transition pore opening: a new paradigm for myocardial preconditioning? Cardiovasc Res.  
596 2002;55(3):534-43.
- 597 54. Yellon DM, Downey JM. Preconditioning the myocardium: from cellular physiology to clinical  
598 cardiology. Physiol Rev. 2003;83(4):1113-51.
- 599 55. Will Y, Dykens JA, Nadanaciva S, Hirakawa B, Jamieson J, Marroquin LD, et al. Effect of the  
600 multitargeted tyrosine kinase inhibitors imatinib, dasatinib, sunitinib, and sorafenib on mitochondrial  
601 function in isolated rat heart mitochondria and H9c2 cells. Toxicol Sci. 2008;106(1):153-61.
- 602 56. Fiala O, Ostasov P, Rozsypalova A, Hora M, Sorejs O, Sustr J, et al. Metformin Use and the  
603 Outcome of Metastatic Renal Cell Carcinoma Treated with Sunitinib or Pazopanib. Cancer Manag  
604 Res. 2021;13:4077-86.



- 605 57. Fumarola C, Caffarra C, La Monica S, Galetti M, Alfieri RR, Cavazzoni A, et al. Effects of  
606 sorafenib on energy metabolism in breast cancer cells: role of AMPK-mTORC1 signaling. *Breast*  
607 *Cancer Res Treat.* 2013;141(1):67-78.
- 608 58. Janjetovic K, Vucicevic L, Misirkic M, Vilimanovich U, Tovilovic G, Zogovic N, et al.  
609 Metformin reduces cisplatin-mediated apoptotic death of cancer cells through AMPK-independent  
610 activation of Akt. *Eur J Pharmacol.* 2011;651(1-3):41-50.
- 611 59. Mogavero A, Maiorana MV, Zanutto S, Varinelli L, Bozzi F, Belfiore A, et al. Metformin  
612 transiently inhibits colorectal cancer cell proliferation as a result of either AMPK activation or  
613 increased ROS production. *Sci Rep.* 2017;7(1):15992.
- 614 60. Ben Sahra I, Laurent K, Loubat A, Giorgetti-Peraldi S, Colosetti P, Auberger P, et al. The  
615 antidiabetic drug metformin exerts an antitumoral effect in vitro and in vivo through a decrease of  
616 cyclin D1 level. *Oncogene.* 2008;27(25):3576-86.
- 617
- 618
- 619

- **Figure Legends** -

620

621 **Figure 1.** Haemodynamic changes in rat hearts Langendorff perfused with 1µM sunitinib ± 50µM  
622 metformin ± 1µM NBTI; mean ± SEM; (A) LVDP, (B) CF, and (C) HR; n = 6 for all groups; \* = p<0.05  
623 for vehicle versus sunitinib; # = p<0.05 for sunitinib versus sunitinib + metformin; \$ = p<0.05 for  
624 sunitinib + metformin versus sunitinib + metformin + NBTI (Sun = sunitinib; Met = metformin).

625

626 **Figure 2.** TTC staining for infarct percentage size of heart tissue following Langendorff perfusion  
627 with 1µM sunitinib ± 50µM metformin ± 1µM NBTI; mean ± SEM; n = 6 for all groups; \*\*\* = p<0.001  
628 vehicle versus sunitinib; # = p<0.05 sunitinib versus sunitinib + metformin; \$ = p<0.05 sunitinib +  
629 metformin versus sunitinib + metformin + NBTI (Sun = sunitinib; Met = metformin).

630

631 **Figure 3.** Western blotting analysis for p-AMPKα and GAPDH protein expression of left ventricular  
632 tissue following Langendorff perfusion with 1µM sunitinib ± 50µM metformin ± 1µM NBTI; mean ±  
633 SEM; n = 7 for vehicle; n = 7 for sunitinib; n = 6 for metformin; n = 7 for sunitinib + metformin; n = 7  
634 for NBTI; n = 7 for sunitinib + metformin + NBTI; p-AMPKα bands standardised to GAPDH. \*\*\* =  
635 p<0.001 vehicle versus sunitinib; # = p<0.05 sunitinib versus sunitinib + metformin; \$ = p<0.05  
636 sunitinib + metformin versus sunitinib + metformin + NBTI (Sun = sunitinib; Met = metformin).

637

638 **Figure 4.** Trypan blue staining for live cell population of isolated cardiac myocytes following 4 h  
639 incubation with 1µM sunitinib ± 50µM metformin ± 1µM NBTI; mean ± SEM; n = 7 for all groups; \*\*\*  
640 = p<0.001 vehicle versus sunitinib; # = p<0.05 sunitinib versus sunitinib + metformin; \$ = p<0.05  
641 sunitinib + metformin versus sunitinib + metformin + NBTI (Sun = sunitinib; Met = metformin).

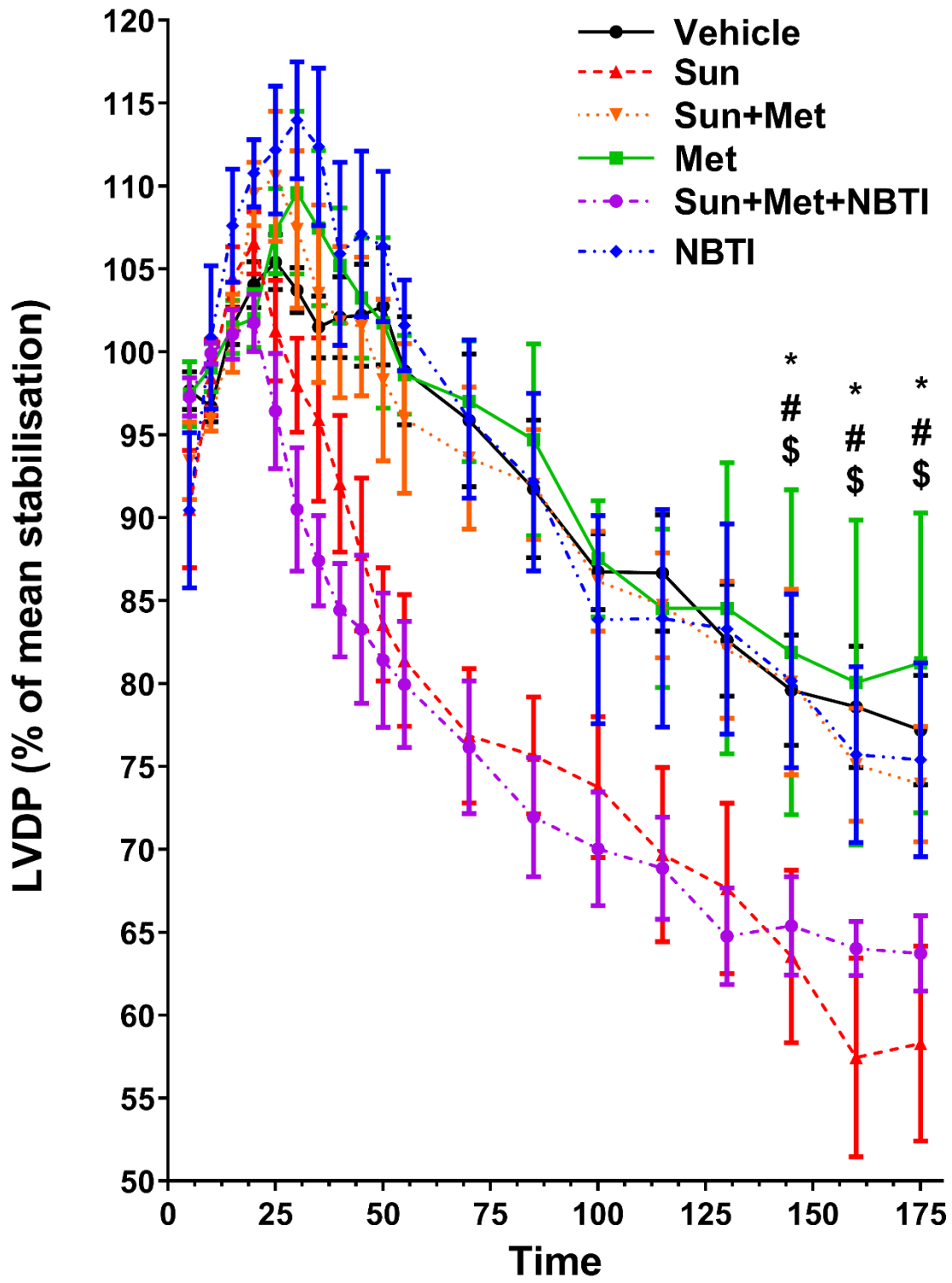
642

643 **Figure 5.** MTT cell viability assay for 0.1-100µM sunitinib ± 50µM metformin in (A) HepG2 cells and  
644 (B) HL-60 cells; mean ± SEM; n = 6 for all groups; # = p<0.05 sunitinib versus sunitinib + metformin  
645 (Sun = sunitinib; Met = metformin).

646

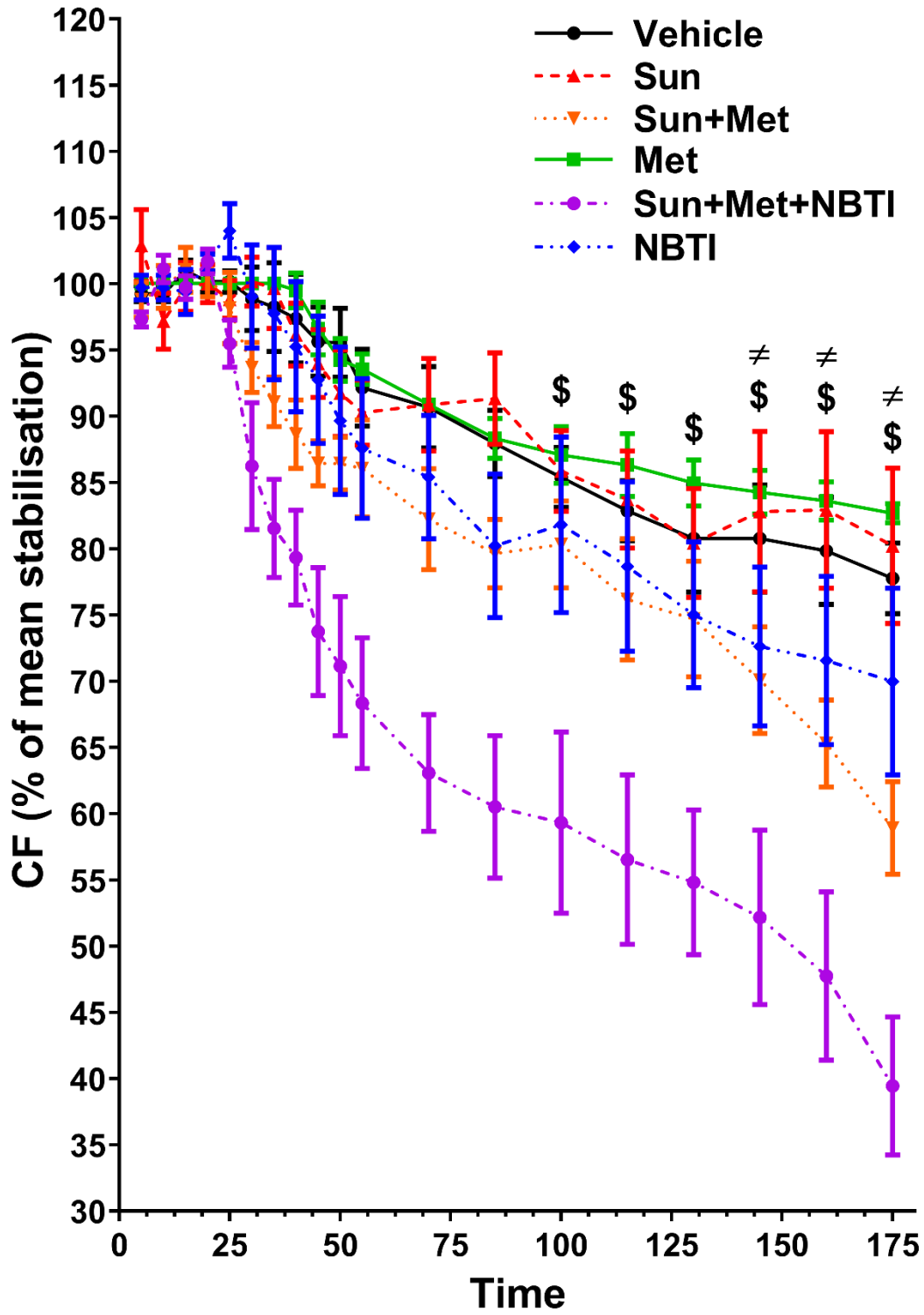
647

648 Figure1A



649

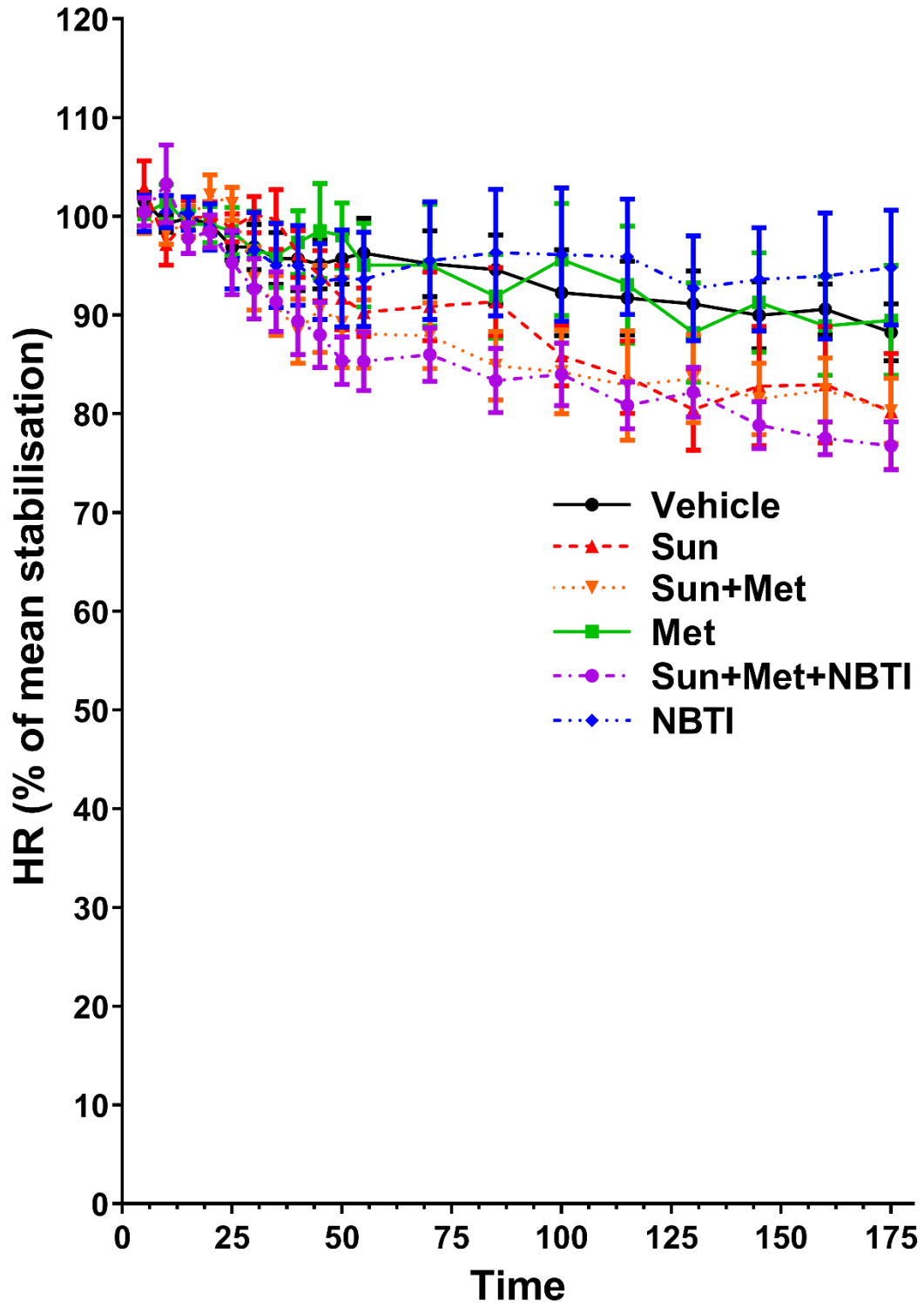
650



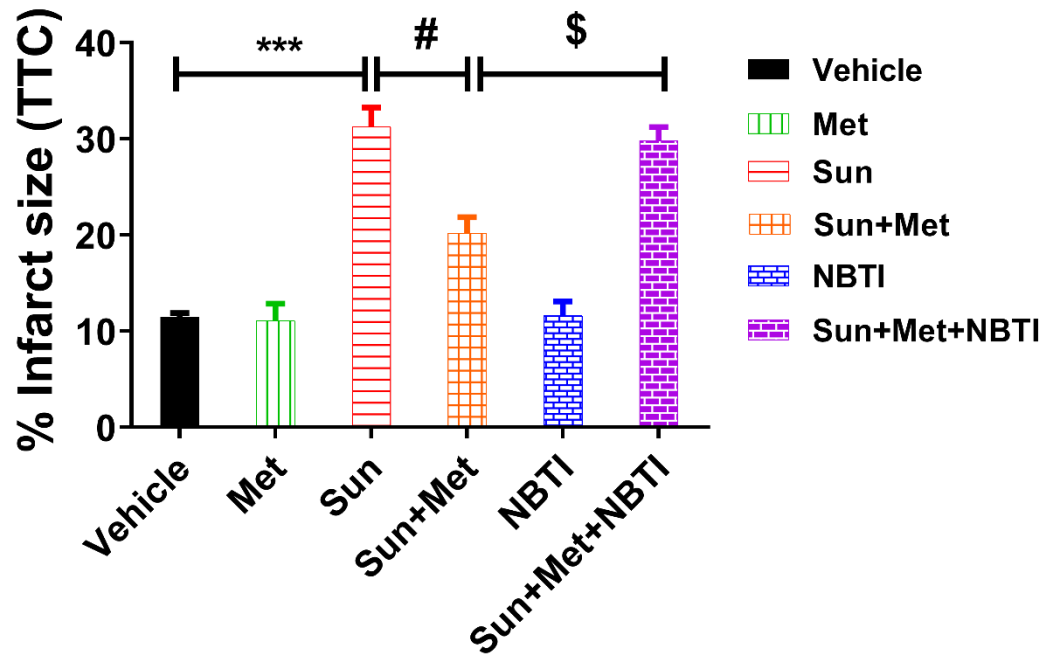
652

653

654



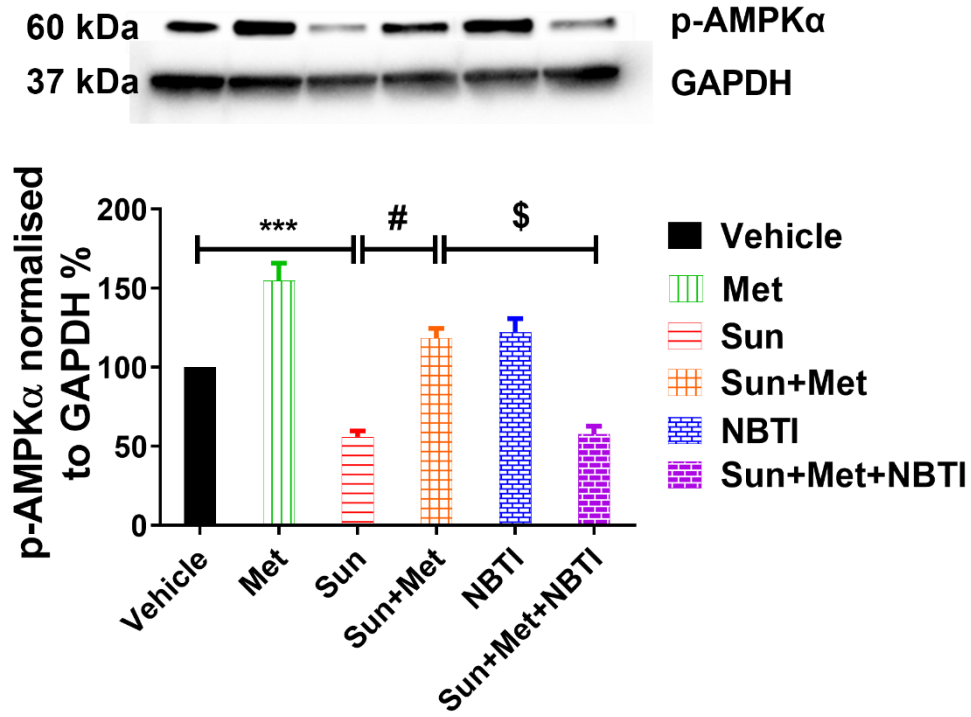
658 Figure 2



659

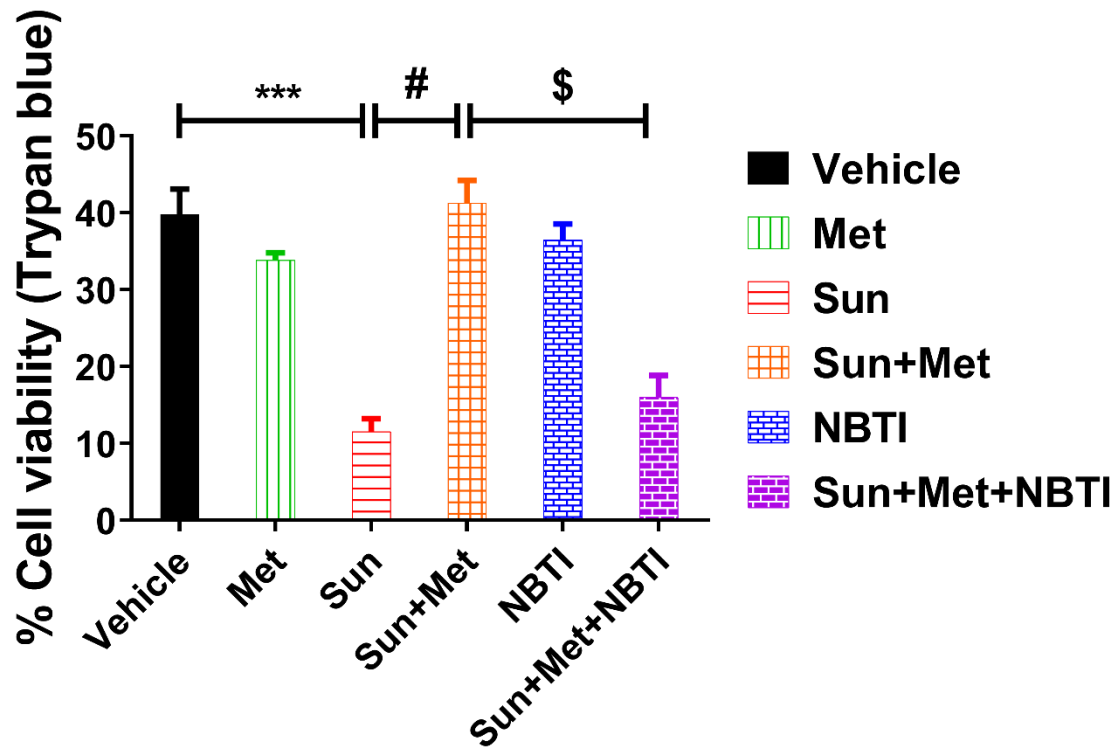
660

661 Figure 3



662

663

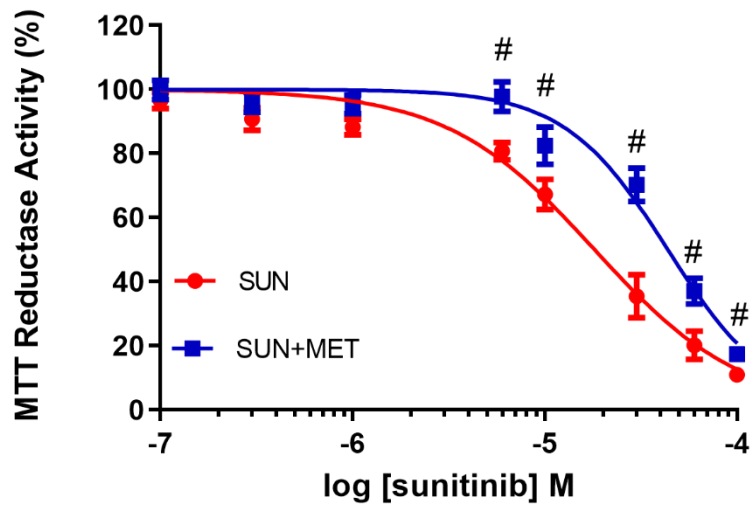


665

666



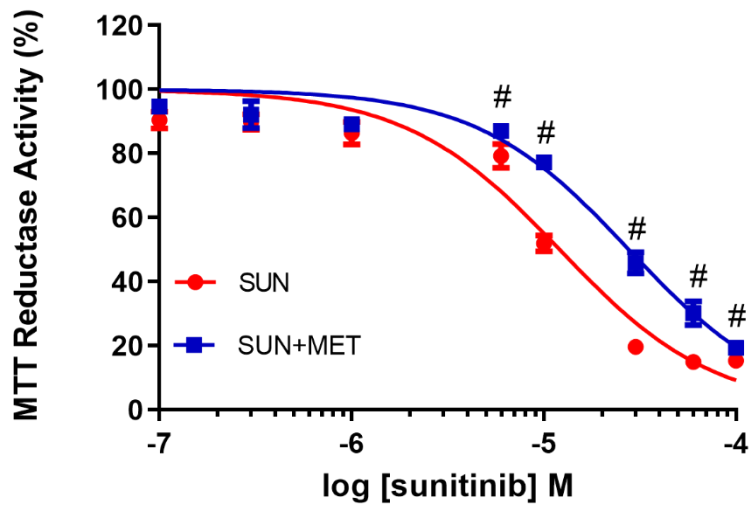
667 Figure 5A



668

669

670 Figure 5B



671